Egyptian Journal of Chemistry

http://ejchem.journals.ekb.eg/

Production of zirconia materials from zircon for dye removal from wastewater

Mohammed Eid M. Ali1, Shimaa M. Abdel Moneim1, Hanan S. Ibrahim1, Nabila S. Ammar1, Heba K. El-Kholly1, Ahmed G. El-Deen2 , M K. Zahran3, and M H. Helal3

Water Pollution Research Department, National Research Center, El-Buhouth St., Dokki, Cairo ² Renewable Energy Science and Engineering Department, Faculty of Postgraduate Studies for Advanced Sciences (PSAS), Beni-Suef University, Beni-Suef and ³Chemistry Department, Faculty of Science, Helwan University, Ain-Helwan, Cairo, Egypt

Zirconia (ZrO2) is a noteworthy metal oxide because of its characteristics. It can be implemented in different applications; adsorption of pollutant, and photocatalytic oxidation. The main focus of this research was to synthesize ZrO2 from low cost and locally available materials; zircon. As well the preparation of ZrO2 was conducted at different temperature procedures. Characterization of prepared materials was performed using X-ray diffraction (XRD), Fourier transform infrared spectra (FTIR) and scanning electron microscope (SEM) which confirmed the production of homogeneous spherical crystalline ZrO2 compared with commercial ZrO2. Moreover, ZrO2-500 was examined for removal of dye using adsorption and photocatalytic activities. The removal adsorptive capacity of ZrO2-500 for red dye 195 was decreased from 37.1 to 2.2 mg/g with increasing dose up to 3 g/L. Meanwhile, red dye was removed with rate constant of 0.132 - 0.324 h-1 under solar simulator. Finally, zirconia was successively prepared from low cost materials with lower energy and materials consumption.

Keywords: Pollutants, zirconia, dye, adsorption, photocatalysis, degradation

1. Introduction

The fabrics coloring procedures usually are associated with the loosing fraction of used dyes that discharged into wastewater effluent. The wasting of dyes is contingent on the characteristic of used dyes in the processing and dyed fabrics. Regarding to azodyes, it is anticipated that through dyeing processes, about fifteen percent of dyes is vanished [1-3]. Annually, about forty percent of used dyes could be discharged to wastewater stream. The protection of water resources from dying effluents has become a serious need [4]. Advanced oxidation technologies (AOTs) have recently been employed to be effective for mineralization of toxic pollutants in wastewater. Among, AOTs, heterogeneous photocatalysis over semiconductor surface is an attractive remediation method which is considered as sludge free wastewater treatment technique **(Badawy et al., 2008; 2015) [5, 6]**. Zirconia-based materials are immensely attractive because of their outstanding thermal stability, chemical resistance, mechanical characteristics, and ionic conductivity [7]. Owing to their excellent characteristic such as high strength, toughness, hardness, wear resistance, and thermal shock resistance, zirconia-based materials are used in many engineering applications including automobile engine parts, wire-drawing dies, and cutting tools. ZrO_2 is an attractive oxide ceramic for thermal barrier coatings on metals and metallic alloys due to its low thermal conductivity and relatively high coefficient of thermal expansion. Additionally, ZrO_2 is an n-type semiconductor with a wide band gap (~5.8 eV), which prohibits its use as an efficient solar photocatalyst. It is well-known that the defect structure has a crucial effect on the physicochemical properties of the metal oxide. The main methods of ZrO_2 doping including metal doping, nonmetal doping, and

co-doping can introduce structural defects into the ZrO_2 structure leading to the adjustment of band gap energy and enhanced visible-light photocatalytic [8-10]. Besides the doping impact, the photocatalytic activity significantly depends on the nanostructural morphology of ZrO_2. Zircon is the most widely distributed and abundant mineral of zirconium. Chemically, zircon is a zirconium orthosilicate ($ZrSiO_4$). Herein, the current targets production of zirconium-based materials from zircon for valorizing the added-value of raw material. As well, feasible and lower cost methodology was applied for production zirconia-based materials and the well known method was upgraded for cost saving; chemical or energy. Therefore, the current work aimed to synthesize and characterize the prepared zirconium-based materials and employed as cost effective substance for decontamination of dyes from waters.

2. Materials and Methods

2.1. Preparation of $ZrO(OH)_2$ from zircon

Predetermined amount of zircon sand obtained and roasted at 150 ᵒC for 1 h to remove the moisture content. Stepwise formation of slurry $ZrO(OH)_2$ precipitate, sodium hydroxide (98%, Fisher Scientific, UK) mixed with zircon using different ratios (zircon : alkali, 1:4) and (zircon : alkali, 1:2) and suspended in 200 mL water. Then, it is followed by heating the mixture at 500 ᵒC with rate 10ᵒC/min in muffle furnace (Nabertherm P330, Germany), and then held for 4 h. The fused mass was cooled to room temperature and then the hot cake that was formed was leached with water and dilute HCl (0.1 N) (Fisher Scientific, UK) and filtered till pH 7.5. The precipitate represents zirconium hydroxide $ZrO(OH)_2$ and the other impurities is soluble in water. Then, the obtained $ZrO(OH)_2$ is washed several times with deionized water to remove the impurities. Then, it is dried in oven (TITANOX, Italy) at 120 ᵒC. The dried powders are grinded and calcinated at 450, 500, and 600 ᵒC to obtain ZrO_2 materials.

2.2. Characterization of prepared materials

X-ray Diffraction (XRD) Analysis

The prepared ZrO_2 materials were examined by XRD technique. The crystallized phases were identified by comparing the collected patterns with standard ASTM cards. XRD patterns were collected using Bruker diffractometer (Germany)

with graphite monochromatized Cu-K$_\alpha$ radiation ($\lambda = 1.5406$ Å).

Fourier Transform Infrared Spectra Analysis

FTIR spectrophotometer (630-JASCO, Japan) was used to determine the differences in functional groups. Pellets were prepared with 2 mg material and 100 mg KBr. The spectra were recorded in the wave number range of 400 to 4000 cm^{-1}.

Scanning Electron Microscope Analysis

The materials were also characterized by the Scanning Electron Microscope using SEM Model Quanta 250 FEG (Field Emission Gun) with accelerating voltage 30 K.V., magnification 14x up to 1000000 and resolution for Gun.

Synthetic wastewater treatment method using prepared materials

Stock solutions for dye (red dye 195) was prepared in deionized (DI) water. It described as the following; to prepare 1000 ppm of dye 1.0 g of dye separately was dissolved in 1 L of DI water.

Adsorption activity of prepared materials

All adsorption trials were conducted on suitable diluted solution of dye under dark conditions. The containers were shaken by shaker (Stuart scientific, UK) at 250 rpm. The solutions of initial and treated samples were filtered through a syringe filter (PTFE, 0.45 μm); also control sample of raw synthetic wastewaters was filtered through the same syringe filter. The residual pollutant in filtrate was analyzed as mentioned below.

The residual dye was measured using spectrophotometric measurements in the ultraviolet and visible regions of the spectrum ranging from 200 to 700 nm were carried out using a JASCO spectrophotometer (Model V730, Japan). All the experiments were conducted in triplicate and the mean of the results were used for further calculations.

The adsorption capacity of ZrO_2 for dye by (q) is estimated according to the following equation (1);

$$q\left(\frac{mg}{g}\right) = \frac{(C_i - C_e)\left(\frac{mg}{L}\right) x\, V}{m\left(\frac{g}{L}\right)} \qquad Eq.(1)$$

The percentage removal of pollutant was calculated according to Eq. (2).

$$\% R = \frac{(C_i - C_e)}{C_i} \times 100 \qquad Eq.\,(2)$$

Where: m is the sorbent mass (g). V is pollutant solution volume (L) in contact with the sorbent. C_i and C_e are the initial and equilibrium pollutant concentration (mg/L), respectively.

Photocatalytic activity for removal of dye

UVCUBE 400 (Honle Technology, Germany) emitting simulated solar light was used as the source of irradiation through all photocatalytic experiments. The intensity of irradiation is 1000 W/m². Dye photooxidation experiments were done in batch mode. Reactive red dye solution was mixed with the desired amount of the ZrO_2 photocatalyst and stirred for 30 min prior to the experiment to allow adsorption equilibrium. The lamp was then switched on to start the photooxidation process. After pre-defined irradiation times, definite volumes of solution were sampled and then filtered (using 0.45 μm PTFE filter) to separate the photocatalyst. The residual dye was measured using spectrophotometer as above mentioned. At maximums wavelength, the absorbance was detected and the dye removal percent was calculated by the following equation (3);

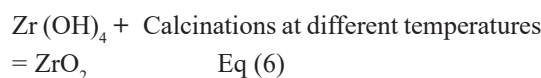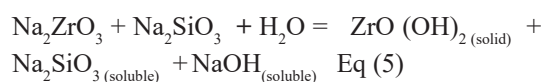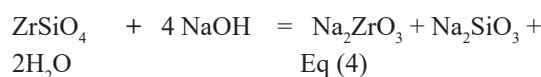$$\% R = \frac{(C_i - C_f)}{C_i} \times 100 \qquad Eq.\,(3)$$

C_i and C_f are the initial and final pollutant concentration (mg/L), respectively.

3. Results and discussion

Production of ZrO_2 materials

For use of zircon as material for zirconium-based materials, it needed to open the zircon. Theoretically, each one mole of zircon required four moles of caustic soda (NaOH), the reaction was taken place at higher temperature and extra-amount of soda. **Manivasakan et al. 2011**, employed higher than five folds of soda amount regarding theoretical value to decompose zircon at temperature of 600 ° C for 3 h [11]. Also previously, zircon material is blended with soda and fused at temperature of 850 °C for 5 h to be decomposed and converted into intermediate products [12] . In the current, the blending ratios of caustic soda and zircon (4:1, and 2:1; soda : zircon) are used and heated at temperature 500 and 600 ºC for 3 h (alkali

fusion). After that, zircon converted to Na_2ZrO_4 associated with Na_2SiO_4 and other impurities as shown in equation (4). Then, the fused materials at different temperature are washed with water to dissolve Na_2SiO_4 and other impurities and finally, ziconyl hydroxide formed as shown in equation (5). Finally, ziconyl hydroxide was calcinated at 450, 500, and 600ºC to form ZrO_2 materials. The current procedure for Zirconium-based synthesis provided reduction energy and materials consumption by 30 % and 40 %, respectively. Therefore, the production cost is reduced on the basis of materials and energy consumption.

$ZrSiO_4$ + 4 NaOH   = Na_2ZrO_3 + Na_2SiO_3 + $2H_2O$ Eq (4)

Na_2ZrO_3 + Na_2SiO_3 + H_2O =   ZrO $(OH)_{2\,(solid)}$ + $Na_2SiO_{3\,(soluble)}$ + $NaOH_{(soluble)}$ Eq (5)

Zr $(OH)_4$ + Calcinations at different temperatures = ZrO_2 Eq (6)

Characterization of prepared materials

XRD analysis results

To confirm the phase formation of ZrO_2 after alkali fusion with NaOH at 500ºC, XRD pattern of the prepared samples were recorded after calcination at 450, 500, 600 º C and is shown in **Figure (1)**. For ZrO_2-450, **Figure (1a)** showed broad and incomplete definite diffraction peaks with remarkable peaks related to zircon. For ZrO_2-500, **Figure (1b)** showed broad and definite diffraction peaks without remarkable peaks related to zircon. It was found the strongest lines at 2Θ of 29.97 º, 21.39, 30.33 and 34 º related for 111 plane of monoclinic phase assigned with standard powder diffraction data using the JCPDS PDF. 81–1314 (monoclinic) and JCPDS PDF. 87–2105 (orthorhombic). Moreover, ZrO_2-600 has mixed phases of monoclinic and orthorhombic ZrO_2. Thus, ZrO_2-500 was selected as model material of monoclinic and orthorhombic ZrO_2. The crystallite size of nanoparticles of ZrO_2 has been calculated by XRD line broadening of using the following formula [13,14].

$$\beta = \frac{k\,\Lambda}{L\cos\theta} \qquad Eq.\,(7)$$

Where, K is 0.9, λ is wave length of X-ray source (0.1540598 nm), β is full width at half maximum in radians, and θ is Bragg´s diffraction angle. ZrO$_2$-500 that calcinated at 500 $^\circ$ C showed good crystalline.

Fig. 1. XRD pattern of different ZrO$_2$ at calcined 450 ° C for 3h (a), 500 ° C for 3h (b), 600 ° C for 3h (c), commercial ZrO$_2$ (d)
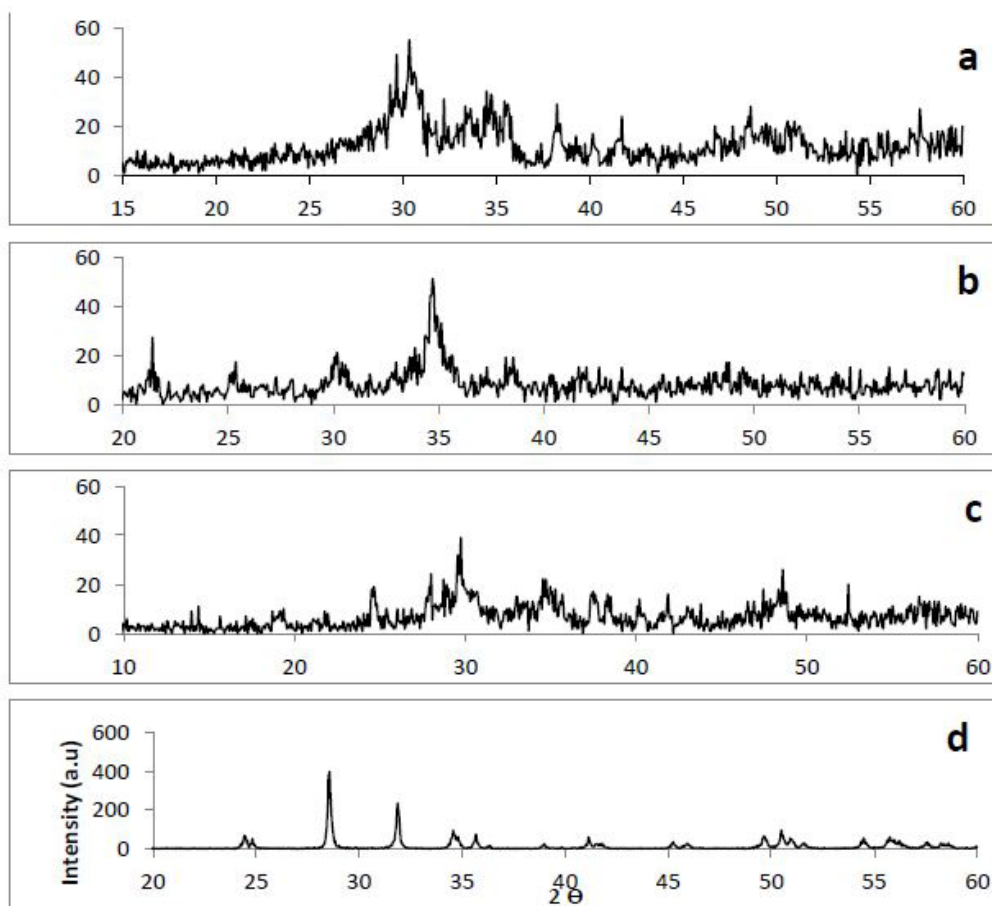
Fourier Transform Infrared (FTIR) analysis

The Fourier transform infrared spectroscopy (FTIR) data were used to verify the functional groups on the nanoparticles. **Figure (2)** showed the FTIR spectra of commercial zirconium dioxide as ZrO$_2$-S reference, and as-prepared ZrO$_2$-500 which was calcinated at 500ºC. There is a remarkable matching of IR bands between reference ZrO$_2$, and as-prepared ZrO$_2$. Common characteristic absorption bands were observed in all two FTIR spectra of samples. IR broad bands were observed between 3020-3680 cm^{-1} and 1620 cm^{-1} are assigned to the stretching and bending vibrations of the O–H bond due to adsorbed water molecules. The peak at 1384 cm^{-1} with low intensity is attributed to the non-bridging OH groups. The sharp and intense IR band was observed at 1033 cm^{-1} that was corresponding to the symmetric vibrations of Zr–O vibrational bands. Meanwhile, a broad intense IR mode between 420-495 cm^{-1} was detected that was corresponding to the asymmetric Zr–O vibrational bands. A broad peak at 684 cm^{-1} is ascribed to Zr–O vibration which is characteristic to tetragonal phase of ZrO$_2$.

Scanning electron microscopy (SEM) of prepared ZrO$_2$-500 materials

To confirm the morphology of prepared ZrO$_2$ materials, the scanning electron microscopy (SEM) was carried out. **Figures (3)** depicted typical SEM images for as-prepared ZrO$_2$-500 materials. SEM image of materials revealed that samples consist of homogeneous assemblies and aggregates of spherical nanoparticles. The obtained SEM imaging results of prepared materials confirmed

the achievement of production of homogeneous   nanocrystalline ZrO_2 from zircon.

Fig. 2. FTIR spectra of prepared ZrO_2-500 materials and reference ZrO_2

Fig.3. SEM of ZrO_2-500 material
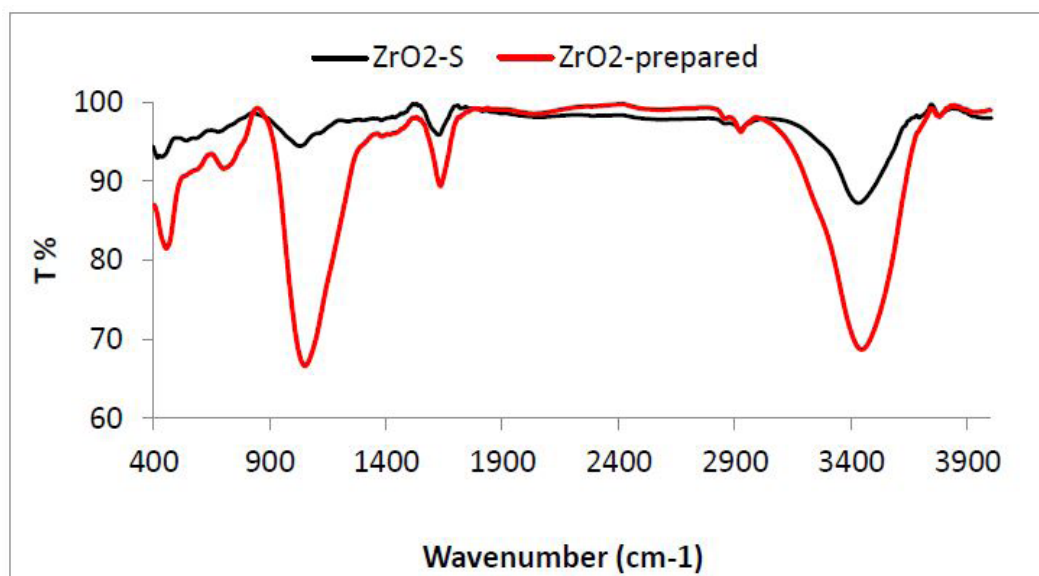
The adsorption efficiency of prepared materials for dye removal

Adsorption capacity of Red dye 195 at 50 mg/L over as-prepared ZrO_2-500 using various doses (0.2 - 3 g/L) was estimated. **Figure (4a)** illustrated the adsorption capacity profile of dye after 30 min contact time. The obtained results showed high to moderate removal efficiency for Red dye 195 at low dose. The results indicated that removal capacity of ZrO_2-500 was decreased from 37.1 to 2.2 mg/g with increasing dose up to 3 g/L. The adsorption was attributed to existence of surface hydroxyl group ionization on ZrO_2 surfaces is the simplest version of multi-site surface complexation models, which may chemically reacts with dye molecule. The decreasing of adsorption of adsorption capacity with higher dose is assigned to the blocking of active site by agglomeration of adsorbent. The extra dose of ZrO_2 results in low dispersion of adsorbent and reduction in available active sites. Nevertheless, the noted reduction of adsorption efficacy for dye uptake with rising of adsorbent amount is mostly owed to the agglomerating and wrapping of active position at elevated adsorbent concentration, which accompany to the decline of the efficient surface area for dye uptake **[15-18]**. **Figure (4b)** showed the reliance of adsorption capacity of dye on dose of ZrO_2-500. It was revealed good relation of dose on dye capacity removal with correlation coefficient R^2 of 0.995.

**Fig. 4. Adsorption removal of red dye from wastewater using ZrO_2-500 (Conc. of dye 50 mg/L)**
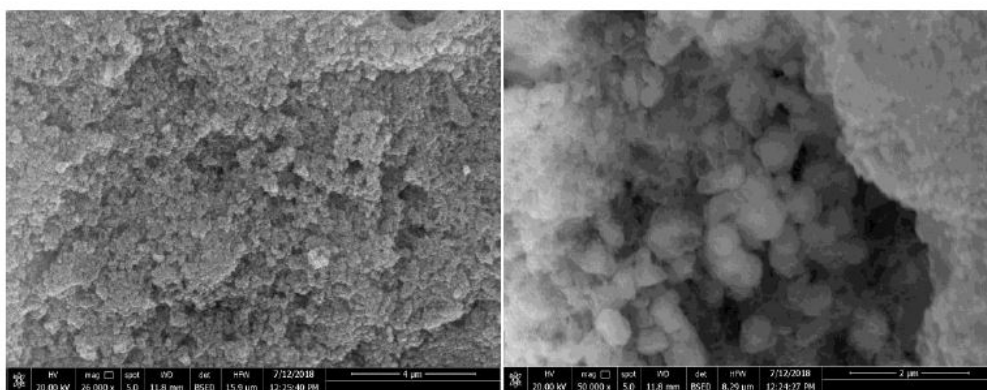
Photocatalytic processes efficiency of prepared materials for removal of dye under sunlight simulator after adsorption

The control trials for adsorption and photolysis were conducted as previously showed. Dye removed via adsorption by 15-30 %. The experimental results showed there is no remarkable removal of dye from wastewater via photolysis under light irradiation. Thus, the presence of light and photocatalyst (ZrO$_2$-500) enhances dye photooxidation. **Figure (5a)** showed the photocatalytic removal of red dye from wastewater using different dose of photocatalyst under simulated sunlight at initial dye concentration of dye of 50 mg/L. Under simulated sunlight, the dye degradation rate was increased with reaction time and with increasing ZrO$_2$-500 dose. It was recorded that the rates of removal after 240 min of irradiation were 34 %, 49 %, 62, 72 % and 60 % for ZrO$_2$ dose of 0.2, 0.4, 0.6, 1.0 and 3.0 g/L, respectively. A decrease in the removal rate of dye was observed for higher concentration of photocatalyst which is probably due to the intervention of mass transfer limitations. Besides, the turbidity, caused by excess photocatalyst, reduced the light transmittance inside the solution leading to lower light intensity reaching the catalyst surface **[6]**. **Figure (5b)** showed kinetic reaction of dye removal using different doses of ZrO$_2$-500, the results revealed that the experimental data are well fitting with first order kinetic reaction with rate constant value range 0.132 to 0.324 h^{-1} (See Table 1). Also, the half life time and initial removal rate of dye are illustrated in Table 1.

Fig. 5. Time profile of dye removal from wastewater over ZrO$_2$-500 (initial Conc. of dye 50 mg/L) combined photocatalytic/adsorption processes
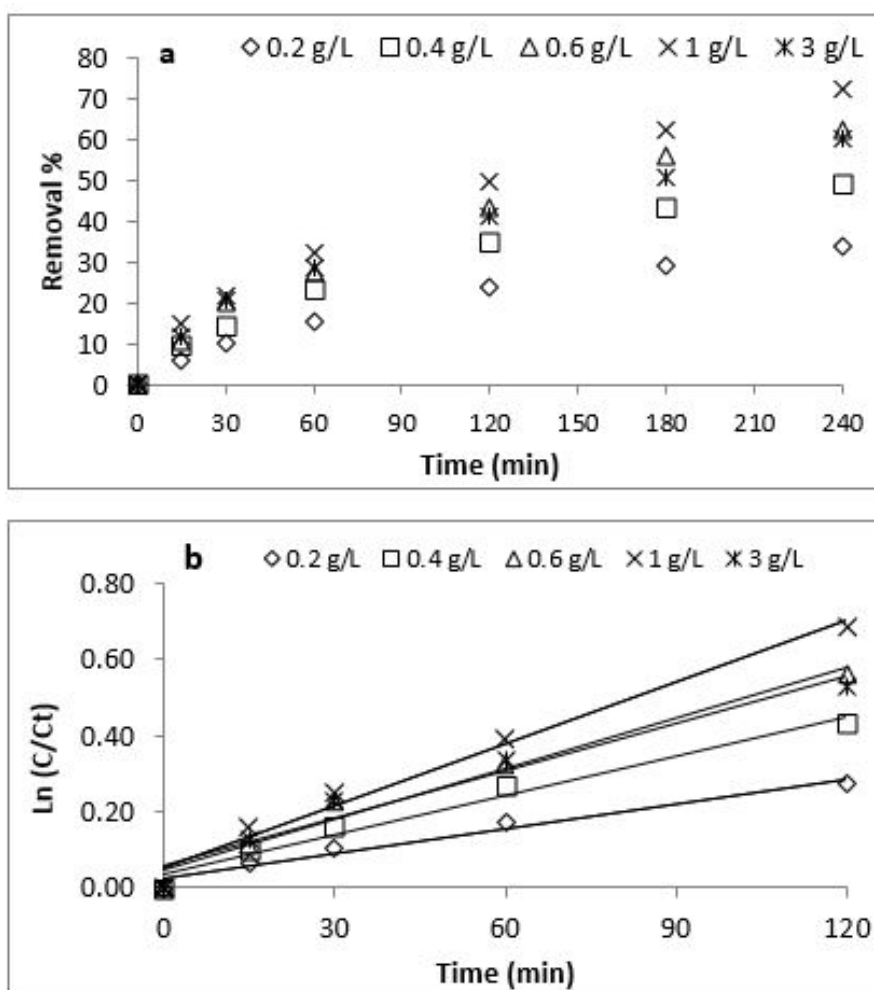
Table 1 First order rate constant (k), reaction rate (r_0) and half life time ($t_{1/2}$) of dye removal

Catalyst dose (g/L)	First order rate constant (k) ,(h^{-1})	Dye removal reaction rate (r_0), (mg. $L^{-1}.h^{-1}$)	Half life time ($t_{1/2}$), (h)
0.2	0.132	6.6	5.3
0.4	0.204	10.2	3.4
0.6	0.27	13.5	2.6
1	0.324	16.2	2.1
3	0.246	12.3	2.8

The dye decontamination by an integrated adsorption and photocatalysis process was also scrutinized to demonstrate the effectiveness of ZrO_2-500. Dye was eliminated by 15-30 % and 34-72 % under condition adsorption in dark and combined adsorption-photocatalytic, respectively (**Figure 6**). Compared with a succession adsorption-degrading process, the integrating adsorption-degradation process had higher efficiency. ZrO_2-500 has dual excellent adsorbent, and photocatalyst properties and accelerating the photocatalysis process as well as enhancing the decontamination of dye. **Figure 7** showed the impact of ZrO_2-500 dose on first order apparent rate constant (k) of dye removal, it is worthy noted that there is a high significant relation between k and dose with R^2 of 0.98 which is characteristics for heterogeneous photocatalysis process.
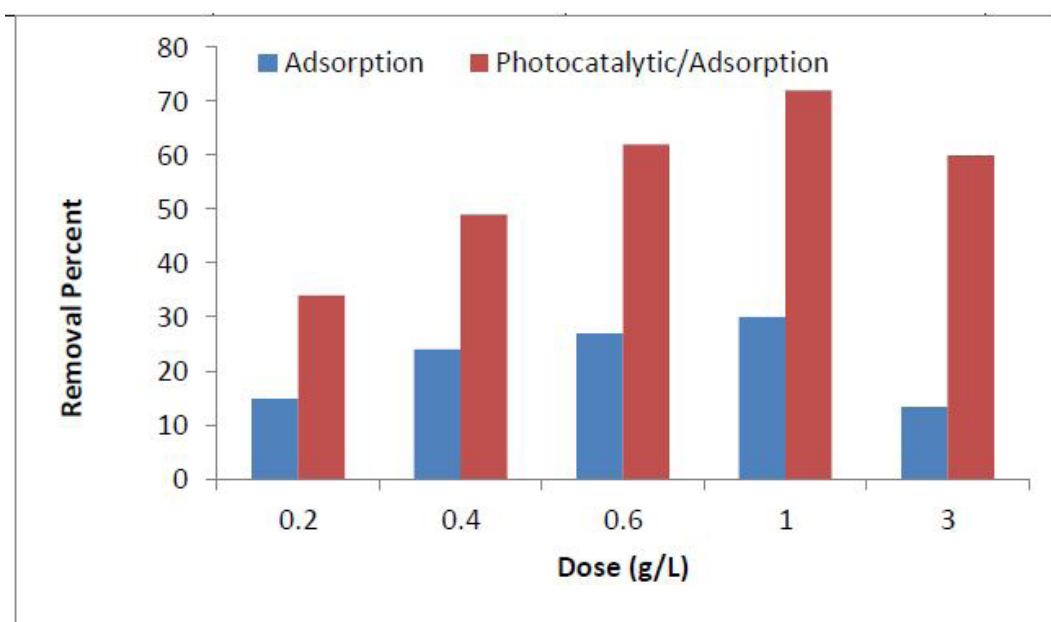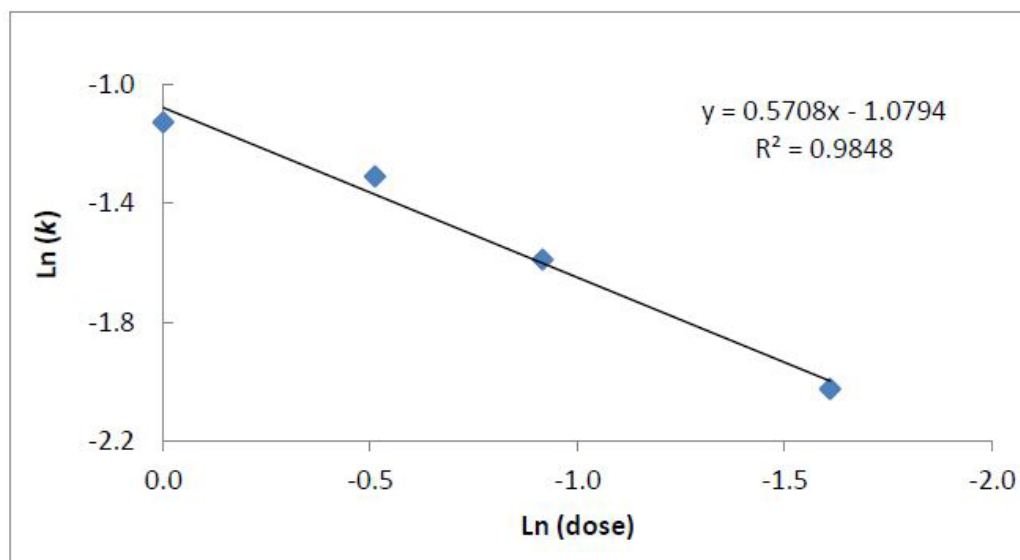
Fig. 6. Removal of dye from wastewater over ZrO_2-500 by adsorption and combined photocatalytic/adsorption processes

Fig. 7. Effect of catalyst dose on first order reaction rate constant of dye removal

4. Conclusions

Zirconia (ZrO_2) was prepared from locally available material (zircon), and it was implemented in different applications; adsorption of pollutant and photocatalytic removal processes. As well, tens grams scale preparation of ZrO_2 from zircon with different ratio; was successfully achieved. Moreover, the activity of different prepared materials for removal of dye was investigated using adsorption and photocatalytic process. The obtained XRD results of prepared materials confirmed the achievement of production of crystalline ZrO_2 from zircon as low cost materials. Also, the crystallite size of prepared materials was estimated and found with range from 28.5 to 47.5 nm. Meanwhile, the analogue of commercial ZrO_2 was 90 nm. FTIR spectra analysis of prepared materials were compared with commercial ZrO_2-S. Moreover, the SEM imaging of prepared ZrO_2-500 showed fabrication of homogeneous spherical crystalline ZrO_2 from zircon. ZrO_2-500 showed adsorption removal of Red dye 195 with capacity of 37.1 to 2.2 mg/g. In addition, photocatalytic activity of ZrO_2-500 material investigated for removal of red dye under sunlight simulator. ZrO_2-500 has limited photocatalysis activity, where It was recorded that the rates of removal after 120 min of irradiation were 23 %, 35 %, 43, 49 % and 41 % for different dose of ZrO_2-500. ZrO_2-500 has dual excellent adsorbent, and photocatalyst properties and accelerating the photocatalysis process as well as enhancing the decontamination of dye.

5. References

1. Chequer FMD, Dorta DJ, de Oliveira DP. Azo dyes and their metabolites; does the discharge of azo dye into Rijeka, Croatia water bodies represent human and ecological risks? In P. Hauser (Ed.), Advances in treating textile effluent (ch.2, pp. 28–48). INTECH, 2011.

2. Ghaly AE, Ananthashankar R, Alhattab M, Ramakrishnan VV. Production, characterization and treatment of textile effluents: a critical review. Journal of Chemistry Engineering Process Technology. 2014; 5(1):1–19.

3. Oliveira DP, Carneiro PA, Sakagami MK, Zanoni MV, Umbuzeiro GA. Chemical characterization of a dye processing plant effluent—identification of the mutagenic components. Mutation Research. 2007; 626(1–2):135–142. doi: 10.1016/j.mrgentox.2006.09.008.

4. Ghaly MY, Ali MEM, Lars Österlund, Khattab IA, Badawy MI, Faraha JY, Zaher FM, Al-Maghrabi MNN. ZnO/spiral-shaped glass for solar photocatalyticoxidation of Reactive Red 120,

Arab. J. Chem. 2017; 10: S3501–S3507.

5. Badawy MI, El Gohary F, Ghaly MY, Ali MEM. Enhancement of Olive Mill Wastewater Biodegradation by Homo-and Heterogeneous Photocatalytic Oxidation. J Hazard. Mater. 2008; 169 (1-3): 673-679.

6. Badawy MI, Ali MEM, Ghaly MY, El-Missiry MA. Mesoporous simonkolleite–TiO$_2$ nanostructured composite for simultaneous photocatalytic hydrogen production and dye decontamination, Process Safety and Environmental Protection. 2015; 94: 11–17.

7. Hui S, Roller JS, Yick X, Zhang C, Decès-Petit Y, Xie R, Maric D, Ghosh A. Brief review of the ionic conductivity enhancement for selected oxide electrolytes, J. Power Sources. 2007; 172: 493–502. http://dx.doi.org/10.1016/j.jpowsour.2007.07.071.

8. Poston MJ, Aleksandrov A B, Sabo DE, Zhang ZJ, Orlando TM, UV photoninduced water decomposition on zirconia nanoparticles, J. Phys. Chem. C. 2014; 118: 12789–12795.

9. Agorku ES, Kuvarega AT, Mamba BB, Pandey AC, Mishra AK, Enhanced visible light photocatalytic activity of multi-elements-doped ZrO$_2$ for degradation of indigo carmine, J. Rare Earths. 2015; 33: 498–505.

10. Zhang J, Li L, Liu D, Zhang J, Hao Y, Zhang W, Multi-layer and open three dimensionally ordered macroporous TiO$_2$–ZrO$_2$ composite: diversified design and the comparison of multiple mode photocatalytic performance, Mater. Des. 2015; 86: 86818–828.

11. Manivasakan P, Rajendran V. Synthesis of Monoclinic and Cubic ZrO$_2$ Nanoparticles from Zircon. J. Am. Ceram. Soc. 2011; 94 (5): 1410–1420.

12. Ozel E, Turan S. Production of coloured zircon pigments from zircon. Journal of the European Ceramic Society. 2007; 27: 1751–1757.

13. Abdel Moniem SM, Ali MEM, Gad-Allah TA, Khalil ASG, Ulbricht M, El-Shahat MF, Ashmawy, AM, Ibrahim HS. Detoxification of hexavalent chromium in wastewater containing organic substances using simonkolleite-TiO$_2$ photocatalyst. Process Safety and Environmental Protection. 2015; 95(5): 247–254.

14. Abdel Moniem SM, Gad-Allah TA, El-Shahat MF, Ashmawy, AM, Ibrahim HS. Novel application of metal-free graphitic carbon nitride (g-C$_3$N$_4$) in photocatalytic reduction—Recovery of silver ions Journal of Environmental Chemical Engineering. 2016; 4(4) Part A: 4165-4172.

15. Wu C. Adsorption of reactive dye onto carbon nanotubes: Equilibrium, kinetics and thermodynamics. Journal of Hazardous Materials 2007; 144: 93–100. http://doi.org/10.1016/j.jhazmat. 2006.09.083.

16. Akbartabar I, Yazdanshenas ME, Tayebi HA, Nasirizadeh N, Investigation of Acid Blue 62 dye adsorption using SBA-15/Polyaniline mesoporous nanocomposite: Kinetic and Thermodynamic study, Iranian Journal of Health Sciences 2017; 5(3): 17-34.

17. Çağlar E, Donar YO, Sinağ A, Biroğul İ, Bilge S, Aydincak K, Pliekhov O, Adsorption of anionic and cationic dyes on biochars, produced by hydrothermal carbonization of waste biomass: effect of surface functionalization and ionic strength. Turk J Chem. 2018; 42: 86 – 99.

18. Almutairi MM; Ebraheim EE; Mahmoud MS, Atrees MS, Ali MEM, Khawassek YM. Nanocomposite of TiO$_2$@Ni-or Co-doped graphene oxide for efficient photocatalytic water splitting, Egyptian Journal of chemistry, 19 March 2019, DOI: 10.21608/EJCHEM.2019.9722.1648.